Progress In Electromagnetics Research M, Vol. 14, 113–121, 2010

ANALYSIS OF EPSILON-NEAR-ZERO METAMATERIAL SUPER-TUNNELING USING CASCADED ULTRA-NARROW WAVEGUIDE CHANNELS

J. Bai, S. Shi, and D. W. Prather

Department of Electrical and Computer Engineering
University of Delaware
Newark, DE, 19716, USA

Abstract—The Epsilon-Near-Zero (ENZ) super-tunneling structure with weakly coupled cascaded ultra-narrow channels is proposed and demonstrated to have notably wider bandwidth than single stage tunneling structure. An extensive parametric study for such structures is performed to investigate the factors which can affect super-tunneling performance. It is found that the coupling between the ultra-narrow channels is required to be weak enough to ensure a continuous super-tunneling band. In addition, electric field in the cascaded channels is enhanced, compared with that in the single channel structure.

1. INTRODUCTION

Metamaterials with permittivity or epsilon near zero (ENZ) have attracted much attention from academic and engineering areas due to their unconventional electromagnetic features which can lead to intriguing potential applications, e.g., transparency and cloaking devices and antenna patterning shaping [1–6]. Dispersion relation of rectangular waveguides was employed to realize an ENZ metamaterial at particular frequencies [7], because effective permittivity is approaching zero when frequency is near waveguide cutoff. With the method proposed by Engheta's group [8], an ultra-narrow waveguide channel connecting two larger waveguide sections, equivalently viewed as a section of the waveguide filled with ENZ metamaterial, exhibits an intriguing phenomenon, which has been experimentally demonstrated that the wave is capable of propagating

Received 2 August 2010, Accepted 19 September 2010, Scheduled 24 September 2010
Corresponding author: J. Bai (jbai@udel.edu).

through the ultra-narrow channel with negligible reflection, i.e., super-tunneling [9]. Moreover, the field intensity in the ultra-narrow channel is dramatically enhanced, thereby providing opportunities for material sensing, e.g., dielectric constant of a material [10]. In addition, the ultra-narrow channels, independent of shape, geometry, length and abruption, can achieve nearly perfect impedance match between two waveguides with negligible reflection, which nevertheless only can be experienced at a single frequency. Besides, signals at frequencies around super-tunneling still can get partially transmitted due to finite height of the channels in reality. However, real applications require ENZ super-tunneling to have a certain bandwidth and prevent useless signal from passing the channel if an additional filter is not wanted. Wider bandwidth and higher stop-band isolation are desired by real applications. To this end, cascaded ENZ metamaterial structures are proposed in this paper. In such structures, more than one ultra-narrow channels connected by waveguide sections are incorporated in a cascading way, thereby introducing mutual coupling between the ultra-narrow channels. Classical equivalent circuit method [11] for cascaded cavities is not well suitable to be directly applied to analyze coupled ENZ channels, because the physical mechanism behind this phenomenon is entirely different with that for conventional coupled Fabry-Perot resonators. As a result, extensive studies are performed to characterize the ENZ structure with the cascaded ultra-narrow channels, especially on field squeezing and super-tunneling bandwidth. Simulations are performed by Ansoft 3D High Frequency Structure Simulator (HFSS) based on finite element method (FEM).

In the next section, the factors which enable us to adjust the bandwidth of super-tunneling are investigated. In Section 3, we discuss the features and advantages attained from the proposed structures. Lastly, the conclusion is presented in Section 4.

2. CASCADED ENZ METAMATERIAL SUPER-TUNNELING

2.1. One-stage ENZ Metamaterial Super-tunneling

The wave propagation of dominant TE_{10} mode in a rectangular waveguide can be equivalently described as a planar wave in the medium with an effective relative permittivity

$$\varepsilon_{r,eff} = \varepsilon_r \left[1 - \left(\frac{\lambda}{2a}\right)^2\right] \tag{1}$$

where a is the width of a waveguide, ε_r is the relative permittivity of material filled in the waveguide, and λ is wavelength. As seen from (1), the effective permittivity of ε_r is near zero when λ approaches the cutoff wavelength of $2a$. Therefore, ENZ metamaterial can be realized by waveguides operating at the cutoff, as shown in Fig. 1. An ultra-narrow channel with the height of b_1 and the length of L_1 is applied to connect two X-band rectangular waveguides with the width of $a = 22.86\,\text{mm}$ and the height of $b = 10.16\,\text{mm}$. Super-tunneling takes place at the frequency which is estimated using the cutoff frequency of TE_{10} mode of the ultra-narrow channel with the width of a_1, the height of b_1 and the length of L_1. In the case of $a_1 = 16\,\text{mm}$, the cutoff frequency of f_{ch} is 9.375 GHz. Super-tunneling of this structure is observed at about 9.3 GHz. The small disagreement is caused by parasitic capacitance induced by the discontinuity in E-plane [12]. To find the relation of b_1 and L_1 with super-tunneling bandwidth, an extensive parametric study is performed. First, by maintaining $b_1 = 1.5\,\text{mm}$ and varying L_1,

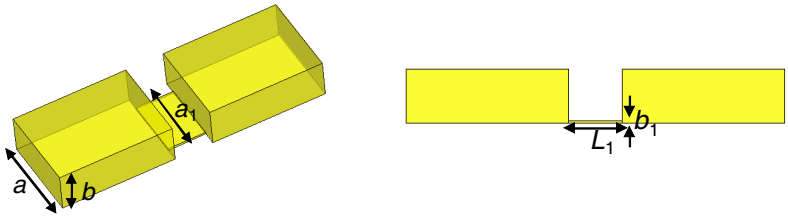

Figure 1. Geometry of one-stage ENZ super-tunneling structure: perspective view and side view. The ultra-narrow channel connects two standard X-band waveguides.

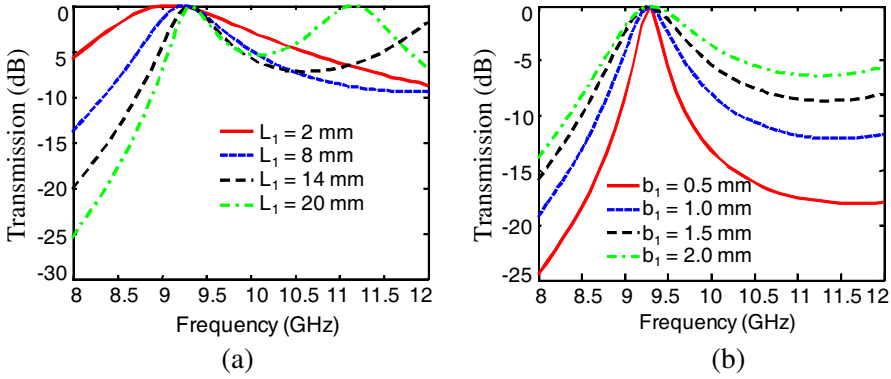

Figure 2. One-stage ENZ tunneling: (a) maintain $b_1 = 1.5\,\text{mm}$ to vary L_1 from 2 mm to 20 mm; (b) maintain $L_1 = 20\,\text{mm}$ to vary b_1 from 0.5 mm to 2.0 mm.

the tunneling strength around 9.3 GHz gets enhanced as L_1 decreases, as illustrated in Fig. 2(a). An opposite conclusion regarding b_1 is obtained by maintaining L_1 to be 20 mm and varying b_1, as illustrated in Fig. 2(b). However, the super-tunneling with negligible reflection only takes place in the very narrow region. The second peak which appears at about 11.2 GHz in Fig. 2(a) when $L_1 = 20$ mm is due to the Fabry-Perot resonance. In addition, the results from the one-stage structure in good agreement with other published results can verify validity of our simulations [8, 9].

2.2. Cascaded Three-stage ENZ Metamaterial Super-tunneling

Wide bandwidth of super-tunneling can be achieved by cascaded multiple stage structures. The geometry of a three-stage structure, as illustrated in Fig. 3, is the three ultra-narrow channels connected by two waveguide sections. The length, width and height of the three ultra-narrow channels are represented as (a_1, L_1, b_1), (a_2, L_2, b_2), (a_3, L_3, b_3), respectively. The two short waveguide sections with the length of L_{wg1} and L_{wg2} have the same cross-section as the feeding and output waveguide. To obtain clear conclusions, we enforce $L_1 = L_2 = L_3 = L_{ch}$, $b_1 = b_2 = b_3 = b_{ch}$, and $L_{wg1} = L_{wg2} = L_{wg}$ in the following analysis. First, we investigate how the length of the connection waveguides affects bandwidth of the three-stage ENZ metamaterial super-tunneling. Then, maintain $L_{ch} = 10$ mm and vary L_{wg} from 6 mm, 8 mm, 10 mm, and 12 mm, respectively. As shown in Fig. 4(a), there is no evident change in the bandwidth with various L_{wg}, except for the shift along the frequency axis. In addition, the length of the ultra-narrow channels can influence the bandwidth as well. In

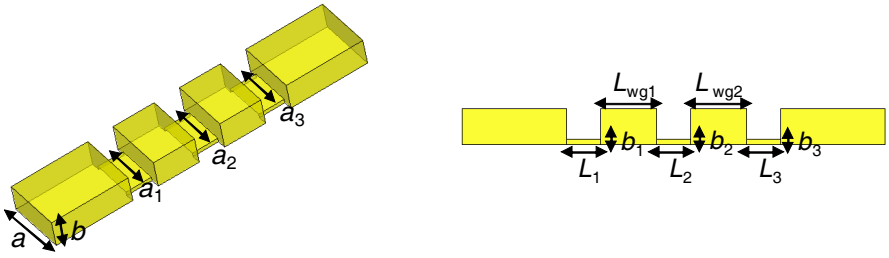

(a) (b)

Figure 3. Geometry of cascaded three-stage ENZ tunneling configuration: (a) perspective view; (b) side view. The three ultra-narrow channels are connected by two standard X-band waveguide sections.

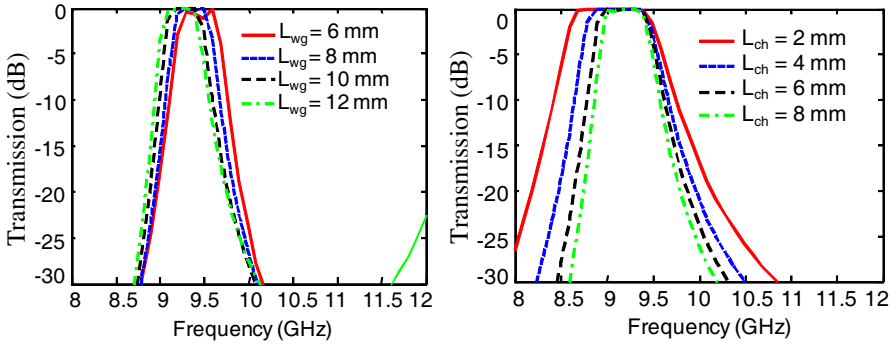

Figure 4. Transmission of the cascaded three-stage super-tunneling structure. (a) Maintain $L_{ch} = 10\,\text{mm}$ to vary L_{wg} from 6 mm to 12 mm; (b) maintain $L_{wg} = 12\,\text{mm}$ to vary L_{ch} from 2 mm to 8 mm.

Table 1. The geometric parameters for the one-stage and cascaded three-stage ENZ super-tunneling structure (unit: mm).

a	b	a_1, a_2, a_3	b_1, b_2, b_3	L_{wg1}, L_{wg2}	L_1, L_2, L_3
22.86	10.16	16	1.5	12	8

Fig. 4(b), we keep $L_{wg} = 12\,\text{mm}$ and vary L_{ch} from 2 mm, 4 mm, 6 mm, and 8 mm. As a result, the shorter ultra-narrow channels can give wider bandwidth of super-tunneling. The geometric parameters of the one-stage and three-stage structures are listed in Table 1. Super-tunneling of the one-stage structure is expected to be at 9.3 GHz and that of the three-stage at about 9.0 GHz–9.4 GHz. The following discussion is based on the analysis of the simulation results of these structures.

3. DISCUSSION

The cascaded multiple stage ENZ tunneling structure can be operated under two different kinds of modes, i.e., ENZ super-tunneling mode and Fabry-Perot resonant mode, similar to the one-stage structure. The operating mode can be identified by the field distributions. Fig. 5 is the electric fields in the middle plane along the waveguide respectively operated under the two modes. As seen from the Fig. 5(a), strong and uniform electric field is excited in all of the ultra-narrow channels of the three-stage structure operated under super-tunneling mode at 9.3 GHz. The strong field excited around the region of intersection between waveguides and channels is due to the abrupt discontinuity

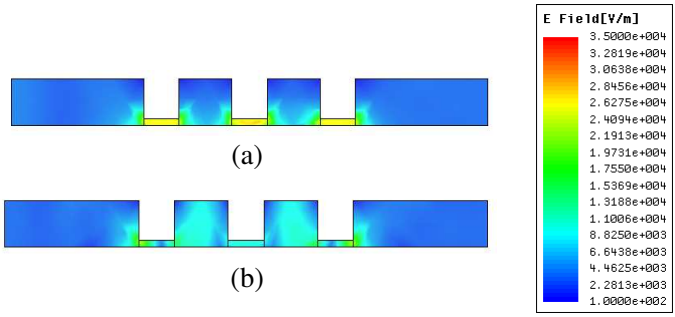

Figure 5. The field distribution of two different modes: (a) ENZ super-tunneling mode at 9.3 GHz; (b) Fabry-Perot resonant tunneling mode at 13.7 GHz.

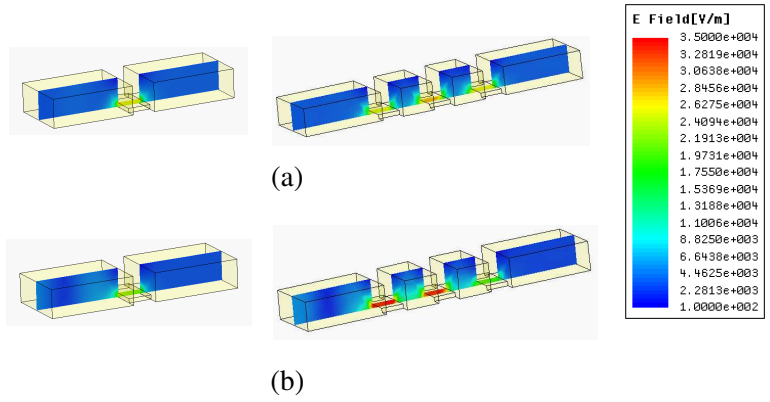

Figure 6. The field distribution of one-stage and three-stage structure under super-tunneling mode, respectively at: (a) 9.3 GHz; (b) 9.0 GHz.

in E-plane. As a comparison, the electric field, displayed in Fig. 5(b) observed at 13.7 GHz under Fabry-Perot mode, has a quasi-sinusoidal distribution. Then, a close examination is worth being performed on the field distribution of the three-stage structure at other different frequencies in the super-tunneling band of 9.0–9.4 GHz. Fig. 6 shows the electric field distribution at 9.0 GHz and 9.3 GHz, respectively. As seen from Fig. 6(a), the electric field at 9.3 GHz in the three-stage structure is still uniform in each channel, which is, however, not really true at 9.0 GHz. As shown in Fig. 6(b), even though uniform in every individual channel of the three-stage structure, the field amplitude of about 3.5×10^4 V/m in the left and middle channel is nevertheless as twice as that in the right channel. It is also observed that the field in the left and middle channel of the three-stage structure is much

stronger than that in the channel of the one-stage. It means, at some frequencies, even after the field has been squeezed from the waveguide sections into all of the ultra-narrow channels by well-known super-tunneling, the field in these channels is squeezed once again between each other, e.g., from the one into the other two or from the two into the other one. The specific field squeezing way is dependent on frequencies in the super-tunneling band. This is due to mutual coupling introduced by the cascaded ENZ structure. Therefore, such phenomenon is unique to multiple stage ENZ tunneling structure, offering much stronger field in the specific ultra-narrow channel and therefore higher sensitivity when applied to sensing.

Another notable advantage of the cascaded ENZ structure is their enhanced super-tunneling bandwidth. The length of ultra-narrow channels is of significance to the bandwidth. As seen from Fig. 4(b), the shorter ultra-narrow channels offer wider super-tunneling bandwidth. In addition, changing the length of L_{wg} enable us to slightly adjust super-tunneling band location. We can see from Fig. 4(a), the band shifts towards the lower frequencies as L_{wg} increases. In addition, as the ultra-narrow channels are close, e.g., $L_{wg} = 6\,\text{mm}$, a split is observed in the flat top of the transmission response. This is due to the coupling which is expected to be stronger as the connection waveguides become shorter. In order to achieve an ideal continuous band of super-tunneling, the coupling between the ultra-narrow channels should be weak enough. As a result, the ENZ tunneling structure with weakly coupled cascaded ultra-narrow channels can provide a wider bandwidth of super-tunneling than the single stage structure.

The super-tunneling of the multiple stage ENZ structure is

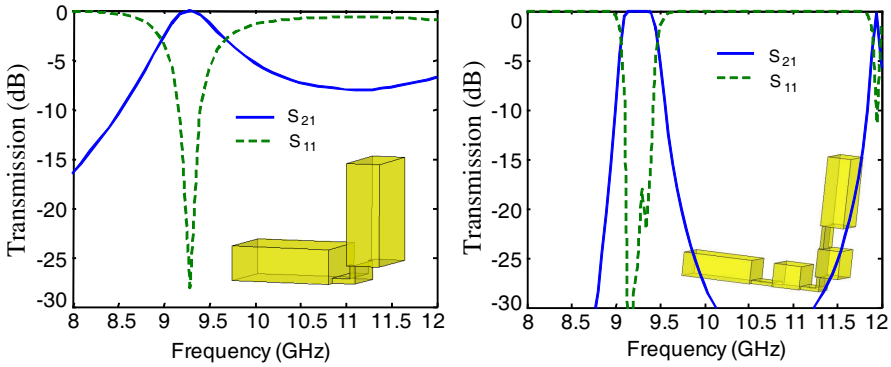

Figure 7. The ENZ super-coupling structure with a 90 degree turn: (a) one-stage; (b) three-stage.

independent of shape, geometry, length and abruption of the ultra-narrow channel. Fig. 7 shows the transmission characteristics of the one-stage and three-stage structure consisting an ultra-narrow channel with a 90 degree turn. As shown in the Fig. 7(a), the one-stage structure has full transmission only at 9.3 GHz and insertion loss of −4 dB at 9 GHz, while the three-stage yields 300 MHz full transmission band from 9.1 GHz to 9.4 GHz and the insertion loss of −15 dB at 9 GHz. As a result, wider bandwidth, higher stop-band isolation, and extremely low reflection can be obtained by using the three-stage structure as a connector with arbitrarily shaped channels. Further enhanced bandwidth if necessary is achievable as discussed in Section 3, i.e., by adjusting the channel length.

4. CONCLUSION

The ENZ super-tunneling structure with weakly coupled cascaded ultra-narrow channels is proposed and analyzed. The notable advantages of such structures are demonstrated. First, electric field in the part of ultra-narrow channels is enhanced at the specific frequencies. Secondly, wide bandwidth of super-tunneling can be obtained and controlled by the length of connection waveguides. In addition, the coupling between the channels should be very weak to ensure a continuous super-tunneling band. Some ENZ-based applications get opportunities to have their performance improved by using the multiple stage structure. For example, the channel with stronger field leads to the application of high sensitive material sensing. In addition, extremely low insertion loss waveguide connection can be implemented with wide bandwidth instead of a single frequency. Wideband ideal coax-to-waveguide impedance matching [13] is also achievable if the influence on input impedance imposed by the connection waveguides is taken into account.

REFERENCES

1. Marques, R., F. Martin, and M. Sorolla, *Metamaterials With Negative Parameters: Theory, Design and Microwave Applications*, Wiley Series in Microwave and Optical Engineering, Wiley, New York, 2008.
2. Weng, Z. B., X. M. Wang, and Y. Song, "A directive patch antenna with arbitrary ring aperture lattice metamaterial structure," *Journal of Electromagnetic Wave and Applications*, Vol. 23, No. 13, 1763–1772, 2009.

3. Alu, A., F. Bilotti, N. Engheta, and L. Vegni, "Theory and simulations of a conformal omnidirectional sub-wavelength metamaterial leaky-wave antenna," *IEEE Trans. Antennas Propag.*, Vol. 55, No. 6, Pt. 2, 1698–1708, Jun. 2007.
4. Pacheco, J., T. Gregorczyk, B. I. Wu, and J. A. Kong, "A wideband directive antenna using metamaterials," *PIERS Proceedings*, 479, Honolulu, HI, Oct. 13–16, 2003.
5. Alu, A., M. G. Silveirinha, A. Salandrino, and N. Engheta, "Epsilon-near-zero metamaterials and electromagnetic sources: Tailoring the radiation phase pattern," *Phys. Rev. B*, Vol. 75, 155410, Apr. 11, 2007.
6. Zhou, H., Z. Pei, S. Qu, S. Zhang, J. Wang, Q. Li, and Z. Xu, "A planar zero-index metamaterial for directive emission," *Journal of Electromagnetic Waves and Applications*, Vol. 23, No. 7, 953–962, 2009.
7. Rotman, W., "Plasma simulation by artificial dielectrics and parallel-plate media," *IRE Trans. Antennas Propag.*, Vol. 22, 82–84, 1962.
8. Silveirinha, M. and N. Engheta, "Theory of supercoupling, squeezing wave energy, and field confinement in narrow channels and tight bends using epsilon near-zero metamaterials," *Phys. Rev. B*, Vol. 76, 245109, 2007.
9. Liu, R., Q. Cheng, T. Hand, J. J. Mock, T. J. Cui, S. A. Cummer, and D. R. Smith, "Experimental demonstration of electromagnetic tunneling through an epsilon-near-zero metamaterial at microwave frequencies," *Phys. Rev. Lett.*, Vol. 100, 023903, 2008.
10. Alu, A. and N. Engheta, "Dielectric sensing in ε-near-zero narrow waveguide channels," *Phy. Rev. B*, Vol. 78, 045102, Jul. 3, 2008.
11. Pozar, D., *Microwave Engineering*, Wiley, Hoboken, NJ, 2005.
12. Alu, A., M. G. Silveirinha, and N. Engheta, "Transmission-line analysis of ε-near-zero (ENZ)-filled narrow channels," *Phy. Rev. E*, Vol. 78, 016604, Jul. 23, 2008.
13. Alu, A. and N. Engheta, "Coaxial-to-waveguide matching with ε-near-zero ultranarrow channels and bends," *IEEE Trans. Antennas Propag.*, Vol. 58, No. 2, 328–339, Feb. 2010.